J. E. Shepherd, A. Teodorcyzk, R. Knystautas, J. H. Lee 1991 ``Shock Waves Produced by Reflected Detonations'' Progress in Astronautics and Aeronautics 134, 244-264. Correction (Dec 2009) to displayed equation on p. 6.

Shock Waves Produced by Reflected Detonations

J. E. Shepherd
Rensselaer Polytechnic Institute
Department of Mechanical Engineering,
Aeronautical Engineering and Mechanics
Troy, NY USA

A. Teodorczyk, R. Knystautas, J. H. Lee
McGill University
Department of Mechanical Engineering
Montreal, PQ CANADA

August 3, 1989

Abstract

Confined detonations produce a shock wave which repeatedly reflects within the container, producing an unsteady, turbulent, flowfield and slowly decaying as it interacts with its' wake. We report experimental and numerical studies of this phenomenon in planar, cylindrical and spherical geometries. Comparison of one-dimensional numerical simulations and the experimental results suggest that the effective dissipation rates are up to an order of magnitude larger than quasi-steady turbulent channel flow mechanisms would predict. While the wave amplitude decay rates cannot be accurately predicted, most of the qualitative features of the measured pressure waveforms are faithfully reproduced in the numerical simulations. Further experimentation with more ideal vessels and multidimensional simulations including turbulence models are probably required to significantly improve the present estimates.

Introduction

A accidental or deliberate detonation inside a closed vessel will produce a shock wave propagating in the detonation products when the detonation wave reflects from the interior surfaces (walls) of the container. Such reflected waves were observed by LeChatelier and Dixon in early detonation experiments [a] (ca. 1900, described in Bone and Townend, 1927) and are a feature of the numerous experiments conducted since that time. However, the subject has never been closely examined since the detonation has been of principal interest rather than the resulting shock wave.

The reflected shock wave reverberates within the vessel, repeatedly reflecting and slowly decaying in amplitude. Stresses on the vessel produced by the detonation and reflected shock wave are of great practical significance in analyzing the possibility of vessel failure due to accidental or deliberate detonation. Reliable predictions of the

[a] The first observations of reflected detonations were apparently made by Oettingen and Gernet (1888) using a rotating mirror camera.

gas pressure history in this phenomenon are therefore of great interest for explosion hazard analyses. Even in simple vessels, accurate numerical simulation is a challenging problem due to the complex, turbulent flowfield produced by shock-wave boundary layer interactions and instabilities created near the shock focus in cylindrical and spherical geometries.

This paper is an experimental and numerical study of reflected-detonation shock propagation in three simple geometries. First, models for propagating detonations are discussed and an approximate equation of state is constructed. Second, the reflection of an ideal planar detonation wave with a plane wall is considered; ideal and realistic analyses for reflected overpressures are compared. Third, numerical simulation and experimental results are presented for the pressure histories at locations near the interaction of a detonation propagating along a conventional detonation tube (uniform crossection) and the tube endwall. Fourth, the axisymmetric shock wave propagation process in a right circular cylinder vessel is described. Experimental results and numerical simulations are presented for 12 cycles of shock reflection and focussing within the vessel. The effect of dissipation is modeled using turbulent channel flow momentum and energy loss factors. Fifth, similar comparisons are made between experiments and simulations for spherically symmetric shock propagation in a hemispherical vessel.

Ideal Detonation Flowfield

The flowfield produced by an ideal detonation within a closed vessel consists of a constant–velocity, infinitely–thin reactive shock wave (the detonation wave itself) followed by a self–similar isentropic wave (Taylor wave) that brings the fluid set in motion back to rest. Solutions to this problem were obtained independently by Taylor (1950) and Zel'dovich (1942) for the planar and spherical cases. Pressure, density, and temperature distributions behind such an ideal wave is illustrated in Fig. 1 for planar and axisymmetric (cylindrical) propagation. The fluid returns to rest and forms an expanding zone of motionless fluid that extends over about one-half of the distance the detonation has progressed to at any given time. The fluid state immediately behind the detonation wave is approximated as the Chapman-Jouguet state determined by solving the Rankine-Hugoniot equations (conservation of mass, momentum and energy across the wave) with an equilibrium mixture of products moving away from the detonation with a relative velocity equal to the sound speed in the mixture (the Chapman-Jouguet hypothesis).

Extensive experimental observations on gaseous detonations have shown that the real structure is much more complex; a quasi-periodic oscillation of the main detonation wave is coupled to a train of transverse wave disturbances propagating along the detonation front. However, for the purposes of structural loading computations, the idealized CJ wave structure is a good average representation as long as the characteristic detonation oscillation time and length scales are much smaller than those of interest for structural response effects. Experimental measurements behind spherical and cylindrical detonations (Desbordes et al. 1981, 1983) show good agreement with

the calculated profiles based on the Zel'dovich–Taylor model under such conditions. Measurements behind detonations in tubes (Desbordes et al. 1983) reveal a nonideal profile that deviates significantly from the Zel'dovich–Taylor model for the first 13% of the flow behind the detonation and then agrees for the remaining 87% of the flow. The origin and influence of this nonideal flow is described further below.

The characteristic length and time scales associated with detonation oscillation are found to be proportional to the nominal chemical reaction time within the detonation wave. In the present experiments, a very sensitive mixture, stoichiometric acetylene-oxygen ($C_2H_2 + 2.5\ O_2$) at moderate initial pressure (200- 250 torr), with an extremely short reaction time (less than 0.1 μs) was chosen to minimize these nonideal effects. The initial and computed CJ detonation characteristics of the nominal test mixture are given in Table 1. Transverse wave spacings S can be inferred from the critical tube diameter measurements of Knystautas et al. (1982) and the empirical correlation $d_c = 13S$. At 250 torr initial pressure, $d_c \approx 4$ mm which implies that $S \approx .33$ mm.

An ideal reaction zone thickness can be estimated by detailed chemical kinetic modeling (Shepherd et al. 1987) to be approximately 10-20 μm. Significant structure will be observed in the experiments over a much larger distance due to the presence of the transverse waves. Edwards et al. (1976) have shown that the transverse waves will decay in strength by one order of magnitude at a distance of $4S$ (1.2 mm) behind the leading wave. Vasiliev et al. (1972) have also shown that the effective CJ plane (location of sonic flow) occurs at about $20S$ (7 mm) behind the leading wave in stoichiometric acetylene-oxygen at an initial pressure of 230 torr. We conclude that the wave structure is small in comparison to the size of the apparatus (minimum dimensions of 30-100 mm) used in the present experiments.

Characteristic oscillation frequencies produced in the pressure by transverse wave interactions can be estimated as $f_o = U_{CJ}/L$, where L is the cell length, approximately $1.6S$. In the present experiments, $f_o = 4.5$ MHz, corresponding to a period of 0.22 μs. Both the time and length scales associated with the transverse waves are much smaller than could be resolved by the instrumentation in the present experiments. The pressure transducers were 3 mm in diameter and the digitizing sample intervals were all larger than 1 μs.

The pressure waveforms shown in Fig. 1 illustrate a peculiar feature of the ideal detonation model. Gradients of thermodynamic properties are infinite at the point just behind the detonation in cylindrical (and also spherical) geometries. This singular behavior makes the flow in the vicinity of the detonation difficult to accurately simulate with standard finite difference numerical solution methods. In addition, the shock produced when the detonation interacts with the wall will propagate back through this strong gradient. Propagation down a gradient in density results in shock amplification which partially counteracts the attenuation effects of the expansion wave following the shock.

Numerical Simulations

Numerical simulations of the detonation reflection and shock propagation process were performed. These simulations were of the inviscid gasdynamics processes of unsteady fluid motion and shock wave propagation. The effect of turbulent dissipation mechanisms was examined in some cases by adding friction and heat loss terms based on turbulent channel flow correlations. The one-dimensional equations of compressible flow with friction and heat loss are:

$$\frac{\partial \rho}{\partial t} + \frac{\partial \rho u}{\partial x} = 0$$

$$\frac{\partial \rho u}{\partial t} + \frac{\partial \rho u^2}{\partial x} = -\frac{\partial p}{\partial x} - \rho u|u|\frac{C_f}{w}$$

$$\frac{\partial}{\partial t}\rho(e + \frac{u^2}{2}) + \frac{\partial}{\partial x}\rho u(e + \frac{p}{\rho} + \frac{u^2}{2}) = -2\rho|u|c_p(T - T_w)\frac{C_h}{w}$$

The symbols are: ρ, gas mass density; u, gas velocity; p, gas pressure; e, gas internal energy; T, gas temperature; C_f, friction coefficient; C_h, heat transfer coefficient (Stanton number); T_w, wall temperature; c_p, specific heat at constant pressure; w, channel radius or width. These equations were solved by the explicit Flux–Corrected Transport finite-difference method described by Oran and Boris (1986). Computations were carried out on a coarse 100 point uniform mesh when the shock was in the vessel interior and on a 250 point variable mesh when the shock was near the walls or the center of symmetry. The variable mesh was used to increase the spatial resolution by a factor of 10 near the shock reflection or implosion point.

The equation of state for the combustion products was approximated as an ideal gas $p = \rho RT$ and a constant specific heat internal energy $e = c_v T$ was used for simplicity. The value of c_v/R was determined by fitting the internal energy expression to the results of detailed thermochemical computations of the states along the isentrope passing through the CJ point. The STANJAN (Reynolds 1986) chemical equilibrium code and JANNAF data for the product species CO_2, CO, H_2O, H_2, O_2, O, H, HO_2, and H_2O_2 were used in this computation.

Linear regression of e vs. pv determined an effective specific heat ratio $\gamma = 1.1414$. Computed states and the regression fit are shown together in Fig. 2. Note that the fit was determined only over the pressure range of .2 to 2.5 (2 - 25 bars) times the CJ pressure (10.5 bar). This range covers that observed in the experiments but significantly higher pressures are computed near the wave focus and are expected to occur in the experiments. Within the range of the fit, the disagreement between ideal and actual values is never greater than 0.5%.

As shown in Fig. 2, the real energy falls significantly below the ideal value as the pressure is increased above 100 bars, i.e., $pv > 2$ MJ/kg. This effect is due to

dissociation, the temperature is 6070 K at the highest energy point shown on the plot, which corresponds to a pressure of 500 atm. Ionization will begin to play an increasing role and the real energy will fall even lower than the ideal value as the temperature increases above 6000 K . Note that molecular interaction effects are not expected to be significant until much higher pressures are reached. This increasing departure of the real energy from the ideal values is one source of error in simulating the shock motion near the wave focus. Since the actual motion near that point is expected to be multidimensional due to instabilities in the collapse process (Grönig, 1986), the error in thermodynamic state is expected to be a small part of the overall error.

A simple "CJ burn" model was used to simulate detonation propagation in the numerical modeling described below. A constant amount of energy is subtracted from the gas internal energy after passing through the detonation wave. Ahead of the detonation, $x > U_{CJ}t$, the internal energy was $e = c_v T + e_o$; behind the detonation, $x < U_{CJ}t$, the internal energy was just $e = c_v T$. An energy constant of $e_o = 95.25$ MJ/kg was determined by matching the computed CJ conditions using realistic thermochemistry and STANJAN to the analytic one-gamma model (Thompson 1972) results. The value of γ used for both products and reactants is that computed from the fitted value of $c_v/R = 1/(\gamma - 1)$.

This fitting approach for γ and e_o guarantees both the detonation wave propagation model and the one-dimensional gasdynamics of the reflected shock wave are properly reproduced by the numerical simulations except extremely near the wave focus. Variations in specific heats, species concentrations, and molecular weight with thermodynamic state are all accounted for with this method.

Experiments

Experiments were carried out at McGill University with stoichiometric acetylene-oxygen mixtures at 200-250 torr initial pressure. Detonations were initiated by exploding wires in three separate facilities: tubes 0.47 - 2.28 m long and 50 mm in diameter; a cylinder 30.7 mm thick and 287 mm in diameter; and a hemisphere 102 mm in radius. Pressures were measured at several locations with piezoelectric transducers and stored in digital waveform recorders. Measurements were obtained for up to 12 cycles of shock reflection.

Detonations in the cylindrical and spherical experiments were initiated in separate tubes and then allowed to diffract into the main chamber through a small connecting tube. Due to the tube opening at the center of symmetry, the implosion of cylindrical and spherical waves will be incomplete and distorted. Some energy will be directed into the initiator tube and the gas motion within the main vessel and initiator tube will be coupled. These nonideal effects were not modeled in the numerical simulations or quantified in the experiments. Attempts to directly initiate the detonation within the main chamber did not result in clean waveforms. Failure to have an ideal geometry is one of the sources of uncertainty in the present experiments.

Planar Detonation Reflection

When the detonation first reflects as a shock wave from the end of the tube opposite the ignition point, the highest pressures will be obtained. That pressure will be immediately followed by a decay due to the interaction of the shock with the expansion (Taylor) wave following behind the detonation. The initial interaction and pressure-time history near the endwall immediately following reflection are discussed in this section.

The maximum pressure occurring at the moment of reflection can be computed from the Rankine–Hugoniot equations without taking account of the expansion wave. Those computations are analogous to those used for the more usual nonreactive shock reflection. Computations with realistic thermodynamics were carried out with a modified version of the STANJAN code. The resulting reflected detonation parameters are given in Table 1.

An approximate solution for the reflected shock pressure was first obtained by Zel'dovich and Stanyukovich (1948) for a constant-γ ideal gas:

$$\frac{P_3}{P_2} = \frac{5\gamma + 1 + \sqrt{17\gamma^2 + 3\gamma + 1}}{4\gamma}$$

This is a typographical error. The value should be 2. See p. 373 of Stanyukovich, Unsteady Motion of Continuous Media, Pergammon 1960.

where P_2 is the CJ pressure, P_3 is pressure behind the reflected shock and $\gamma = c_p/c_v$ is the ratio of specific heats. The approximations are: 1) the initial pressure ahead of the detonation can be neglected in comparison to the detonation and shock pressures; 2) the ratio of specific heats γ is the same in reactants and products. This result has a very weak dependence on the ratio of specific heats. For nonreacting real gases, $1.67 > \gamma > 1$, and the pressure ratio only varies between 2.5 and 2.65. For the present problem, the value of $\gamma = 1.1414$ in the products and $\gamma \approx 1.3$ in the reactants. Using the product value of γ in the Zel'dovich–Stanyukovich equation, the predicted pressure ratio is 2.598. The value obtained from the more realistic STANJAN computation is 2.505. The difference is due to the finite initial pressure, different product and reactant γ, and chemical equilibrium effects. It is difficult to precisely measure absolute pressures but the present data and that of previous researchers (Desbordes et al. 1983, Nettleton 1987) are consistent with a reflected–to–incident pressure ratio value of 2.5 ± 0.2.

The interaction of the reflected–detonation shock with the following expansion wave is of some interest. The shock will propagate back through the Taylor wave, moving into regions of lower density as it moves away from the wall. This effect will tend to steepen the wave. However, an expansion also follows the reflected shock, which will attenuate the shock. The net effect is attenuation as shown in computed pressure waveforms presented in Fig. 3. The shock pressure quickly decays following reflection and an almost constant amplitude wave is produced by the time the shock reaches the center of the tube.

A remarkable feature of these solutions shown in Fig. 3 is that the thermodynamic state between the shock and the endwall is almost spatially uniform at any given instant

of time. This is also demonstrated by the coincidence (after the reflected wave passes by) of the pressure-time curves at different locations as shown in Figs. 4 and 5. An exactly uniform state was obtained in analytical studies by Stanyukovich (1960) for the case $\gamma = 3$ and he assumed it to be true for arbitrary values of γ in his linearized studies of the fluid motion following detonation reflection. The present results confirm the excellent nature of his assumption and the validity for the full nonlinear solution with a value of γ near 1.

Pressure histories were measured at the endwall and three nearby locations in the 2.28 m long tube. Pressure transducers were located at normalized distances of $x/L =$ 1.0, 0.967, 0.937 and 0.898. Incident and reflected wave measurements are shown in Fig. 4. The results of the numerical simulations (no losses) are shown in Fig. 5. Absolute amplitudes of the measured shock waves do not agree very well with the predictions. However, the measured ratio of reflected to incident wave amplitude are within 10% of the predicted ratios as shown in Table 2.

It is notoriously difficult to get reliable pressure measurements with piezoelectric transducers in a detonation experiment and the failure to obtain agreement between the absolute measured pressure and predictions is not very surprising. This discrepancy appears to be partially removed by comparing relative values (ratios) rather than absolute pressures. Note that the overall features of the experimental pressure histories are in agreement with the computations, but a high level of pressure oscillations (5-20%) are observed behind the detonation and shock waves while the numerical simulations produce very smooth results.

Pressure oscillations behind self–sustaining detonation waves in tubes have been previously observed by Desbordes et al. (1983). These oscillations are associated with nonideal flowfield immediately following the detonation. This nonideal character immediately behind a detonation in a tube is due to the curvature of the detonation front, which is produced by the diverging streamlines associated with the mass sink effect of the thermal boundary layer on the tube walls. The flow behind the curved front is slightly supersonic with respect to the front rather than sonic as in an the Zel'dovich-Taylor model. The interaction of the curved detonation with the wall and the streamline deflection in the following flow result in a system of weak oblique shock waves as described by Fay (1962) and Edwards et al. (1963). These oblique shocks form a traveling wave system and produce the observed pressure oscillations as the waves move across or reflect from the pressure transducers.

Another possible source of pressure fluctuations are transverse velocity fluctuations driven by shock wave–boundary layer interactions. A boundary layer will be produced in the near–wall fluid behind the detonation (Du et al. 1984) just as in the more well-studied case of a shock wave in a tube. While initially laminar, this boundary layer is expected to rapidly become turbulent and then fill the tube to produce a turbulent channel flow. Measurements behind nonreacting shock waves (Smeets and Mathieu 1988) demonstrate that transition occurs within 10 tube diameters for 2000 m/s shock velocities, comparable to the detonation velocities of the present experiments. Smeets

and Mathieu (1988) have measured the velocity fluctuations in turbulent boundary layers behind incident shocks and find fluctuation levels of 1-5 % with characteristic frequencies close to u_2/D, where u_2 is the postshock velocity in the lab frame and D is the tube diameter.

These fluctuation levels are much lower than those produced by the oblique waves but have a characteristic frequency (20 kHz or a period of 50 μs) comparable to that shown in the data of Fig. 4. Note that the relics of detonation instability, transverse shock waves, decay too rapidly (Edwards et al. 1976, Strehlow et al. 1972) and have too high a characteristic frequency (unobservable!) to be the source of the fluctuations in the present experiments.

Another possible source of nonideal behavior and large pressure fluctuations would be boundary layer separation caused by the interaction with the reflected shock wave. Boundary layer separation and bifurcated reflected shock waves are observed (Mark 1958, Strehlow and Cohen 1959) under certain conditions in shock tubes with nonreacting flows. Mark (1958) formulated a simple model which predicts the occurrence of bifurcation: shock bifurcation and boundary layer separation will occur when the pressure jump across the reflected shock exceeds the maximum stagnation pressure possible in the cold boundary layer fluid. Numerical calculation for the present situation reveals bifurcation would not be expected when the detonation first reflects. This is a situation peculiar to detonations and is due to the much lower reflected–shock pressure ratio relative to that which would be produced by reflecting a shock wave of comparable strength. Consideration of the reflected shock motion at later times indicates that bifurcation would not occur until after the shock had reflected from the far end of the tube.

Cylindrical Vessel

A detonation was initiated in a tube, 35 mm dia. and 188 mm long. A connecting tube, 12 mm dia. and 40 mm long joined the initiator tube to the main vessel, a cylinder 30.7 mm thick and 287 mm dia. The detonation entered the cylinder along its' axis, diffracted and reflected from the opposite side to form a cylindrical detonation propagating outward. This detonation reflected from the outer cylindrical wall of the vessel, producing a shock propagating inward.

Experimental pressure vs. time measurements at three locations, $r/R = 0.89$, 0.71, and 0.53 are shown in Fig. 6. After the detonation wave passes, a single shock is observed to repeatedly reflect from the outer wall, propagate inward, converging to the center and emerging after imploding. Detonation and shock both induce a strong flow within the vessel which produces large amplitude oscillations in the pressure. Individual shock waves appear superimposed on this oscillating background pressure. In addition to the main reflecting shock and oscillations in pressure, high frequency waves and other "fine structure" can be observed in the signals. Repeated experiments reveal that most of the fine structure observed in the pressures of Fig. 6 was very repeatable and not merely fluctuations of the type discussed above in the planar case. These features are

absent in the simulation results and are apparently associated with multidimensional waves and the influence of the initiating tube.

The results of a numerical simulation without losses is shown in Fig. 7. General features of the experimental records are well simulated, the main shocks and pressure oscillations appear to be qualitatively correct. None of the finer features in the experimental records are predicted. Note the much slower decay rate predicted in these simulations. The difference in predicted and observed decay rates suggests that turbulent dissipation mechanisms are very important for the long time scales of the present observations. Another possibility is that the implosion process, being singular, is difficult to properly numerically model. However, numerical experiments using different levels of resolution near the origin suggest that the far-field behavior of the shock emerging after the implosion is very insensitive to the spatial resolution and other details of the computation in the implosion region. A third possibility is that the initiator tube at the origin resulted in disruption of the shock symmetry and rapid degeneration of the original one-dimensional flow into multidimensional modes.

Edwards et al. (1970) have observed that proper accounting for losses is needed to obtain correct description of the pressure in the Taylor wave prior to reflection. In that case, they were able to account for their observations by using quasi-one dimensional computations with standard turbulent channel flow dissipation models. The nominal values of the dissipation coefficients used in those computations (and similar investigations for heat transfer behind shock waves) were $C_f = 0.005$ and $C_h = 0.0025$. This corresponds to turbulent flow at a Reynolds number of 10^5.

Simulation of the present experiments with these dissipation models and the standard coefficient values made only a slight difference in the predictions in comparison to the observations. An ad hoc increase in the dissipation coefficient values by a factor of ten yields much better agreement of the simulation with the experiments. The results of that simulation are shown in Fig. 8. We can only conclude that over long times, that is, following multiple reflections of the shock wave, dissipation mechanisms are greatly enhanced by the shock wave–turbulence interactions and possibly, the nonideal nature of the implosion process at the center of the cylinder. The possibility of significant shock–wave turbulence interactions is consistent with the known turbulent nature of the flow and the observation of large–amplitude pressure fluctuations.

Hemispherical Vessel

Experiments were also performed in a hemispherical vessel 102 mm in radius with a stoichiometric acetylene-oxygen mixture. Experimental results are shown in Fig. 9 for pressure vs. time at three locations, $r/R = 1.0$, 0.875, and 0.5. The shock amplitude attenuation rate does not appear to be quite as large as in the cylindrical case. However, the observed attenuation rate is much larger than that predicted by the simulations of an ideal flow shown in Fig. 10. As in the cylindrical case, repeatable fine features are observable on the experimental records that are not predicted by the simulations. At the outer surface ($r/R = 1$), these features have a large amplitude and

seemingly random character. However, repeated experiments show that almost all of these features (and those in the other two signals) are reproducible. The source of these signals has not been clearly identified but the repeatable character strongly indicates that the initiator tube arrangement may be responsible.

Summary

The process of detonation reflection and shock reflection within a closed vessel has been studied both experimentally and numerically. Measured peak reflected detonation pressures are approximately 2.5 times higher than the CJ pressure. This finding is in agreement with both the Zel'dovich–Stanyukovich approximate analysis and a computation using realistic thermochemistry. Numerical simulations without added dissipation provide a satisfactory representation of the pressure waveforms in the region near the endwall following detonation reflection.

The attenuation of the reflected shock wave over 12 cycles of reflection within cylindrical and spherical vessels has been examined. Computations without added dissipation simulate the qualitative features of the measured pressure histories but the quantitative features, shock amplitudes and decay rates, are incorrect. Computations using turbulent channel flow dissipation models have been compared with measurements in a the cylindrical vessel. These comparisons indicate that the nonideal aspects of the experiments result in a much more rapid decay of the shock wave than predicted by the simple channel flow model. Dissipation mechanisms not directly accounted for in the present model include: multidimensional flow associated with transverse shock waves (originating in detonation or shock instability); separated flow due to shock wave-boundary layer interactions; the influence of flow in the initiator tube arrangement; real gas (dissociation and ionization) effects and fluid dynamic instabilities near the shock focus in cylindrical and spherical geometries.

An approximate representation of these nonideal effects can be obtained by using momentum and energy loss terms that are artificially increased by a factor of 10 over the usual turbulent channel flow values. Even this ad hoc increase in dissipation is inadequate to compensate for the evidently very strong dissipation mechanisms at work in these flows. Further experiments in more ideal vessels and more sophisticated numerical simulations will be needed to improve our understanding of these mechanisms.

Acknowledgements

The authors thank N. Manson for pointing out the historical references on reflected detonations and D. Desbordes for discussions on the Zel'dovich–Taylor flow model.

References

W. A. Bone and W. T. A. Townend 1927 **Flame and Combustion in Gases**, Longmans, 163-173 and 517-518.

D. Desbordes, N. Manson, and J. Brossard 1981 Pressure Evolution behind Spherical and Hemispherical Detonations in Gases. *Progress in Astronautics and Aeronautics* **75**, 151-165.

D. Desbordes, N. Manson, and J. Brossard 1983 Influence of Walls on Pressure Behind Self-Sustained Expanding Cylindrical and Plane Detonations in Gases. *Progress in Astronautics and Aeronautics* **87**, 302-317.

X. X. Du, W. S. Liu, and I. I. Glass 1984 Nonstationary Laminar Boundary Layer Induced Behind Blast Waves and Detonation Waves. *Shock Tubes and Waves*, Eds. R. D. Archer and B. E. Milton, 531-542.

D. H. Edwards, T. G. Jones, and B. Price 1963 Observations on oblique shock waves in gaseous detonations. *J. Fluid Mech.* **17**, 21-32.

D. H. Edwards, D. R. Brown, G. Hooper, and A. T. Jones 1970 The influence of wall heat transfer on the expansion following a C–J detonation wave. *J. Phys. D* **3**, 365-376.

D. H. Edwards, A. T. Jones and D. E. Phillips 1976 The location of the Chapman-Jouguet surface in a multiheaded detonation wave. *J. Phys. D* **9**, 1331.

J. A. Fay 1962 The Structure of Detonation Waves. *8th Symp. (Intl.) on Combustion*, 30-40.

H. Grönig 1986 Shock Wave Focusing Phenomena. *Shock Tubes and Waves*, Eds. D. Bershader and R. Hanson, 43–56.

R. Knystautas, J. H. Lee, and C. Guirao 1982 The Critical Tube Diameter for Detonation Failure in Hydrocarbon-Air Mixtures. *Comb. Flame* **48**, 63.

H. Mark 1958 *The Interaction of a Reflected Shock Wave with the Boundary Layer in a Shock Tube*, NACA TM 1418.

M. A. Nettleton 1987 **Gaseous Detonations**, Chapman and Hall, p. 159.

A. von Oettingen and A. von Gernet 1888 *Ann. Phys. Chem.* **33**, 586.

E. S. Oran and J. P. Boris 1987 **Numerical Simulation of Reactive Flow**, Elsevier, 275.

W. C. Reynolds, *The Element Potential Method for Chemical Equilibrium Analysis: Implementation in the Interactive Program STANJAN, Version 3*, Department of Mechanical Engineering, Stanford University, Palo Alto, CA January 1986.

J. E. Shepherd, I. O. Moen, S. B. Murray, and P. A. Thibault 1987 Analyses of the Cellular Structure of Detonations. *Twenty-First Symposium (Intl.) on Combustion*, The Combustion Institute, 1649-1658.

G. Smeets and G. Mathieu 1988 Investigation of Turbulent Boundary Layers and Turbulence in Shock Tubes by Means of Laser Doppler Velocimetry. *Shock Tubes and Waves*, Ed. H. Grönig, 193-200.

K. P. Stanyukovich 1960 **Unsteady Motion of a Continuous Media**, Pergamon, pp. 372-381.

R. A. Strehlow and A. Cohen 1959 Limitations of the Reflected Shock Technique for Studying Fast Chemical Reactions and Its Application to the Observation of Relaxation in Nitrogen and Oxygen. *J. Chem. Phys.* **30**, 257-265.

R. A. Strehlow, A. A. Adamcyzk, and R. J. Stiles 1972 Transient Studies of Detonation Waves. *Astronautica Acta* **17**, 509-527.

G. I. Taylor 1950 The dynamics of the combustion products behind plane and spherical detonation fronts. *Proc. Roy. Soc.* **A200**, 235-247.

P. A. Thompson 1972 **Compressible Fluid Dynamics**, McGraw-Hill, p. 353.

A. A. Vasiliev, T. P. Gavrilenco, M. E. Topchian (1972) On the Chapman-Jouguet surface in multi-headed gaseous detonations. *Acta Astronautica* **17**, 499.

Ya. B. Zel'dovich and K. P. Stanyukovich 1948 Reflection of a Plane Detonation Wave. *Dok. Akad. Nauk.* **61**, 2.

Ya. B. Zel'dovich 1942 Distribution of pressure and velocity in detonation products. *JETP* **12**, 389.

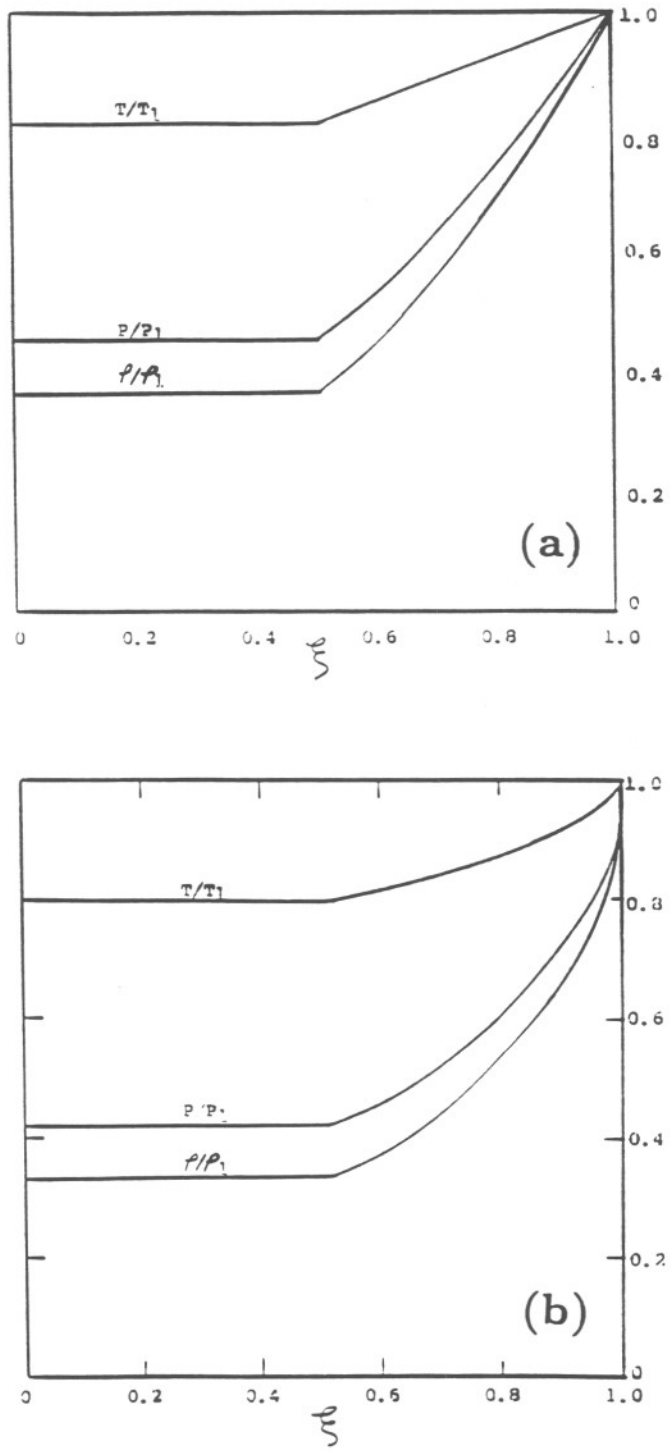

Figure 1. Nondimensional temperature, pressure, and density profiles for a CJ detonation followed by a self-similar isentropic flow (Taylor wave) in (a) planar and (b) cylindrical geometries. Obtained by analytic (planar case) or numerical (cylindrical case) solution of the similarity–transformed equations of motion. The similarity variable $\xi = x/U_{CJ}t$.

Table 1.

Initial conditions, computed detonation and reflected shock properties for the nominal stoichiometric acetylene–oxygen mixtures used in the experiments. Initial pressure is 250 torr and the CJ wave velocity is 2363.4 m/s.

		Initial	Incident	Reflected
P	(atm)	0.329	10.56	26.46
ρ	(kg/m^3)	0.4049	0.7477	1.643
T	(K)	300	3943	4313
e	(MJ/kg)	2.06	2.68	4.05
c	(m/s)	-	1280	1375

Table 2.

Experimental (exp) and calculated (calc) ratios of reflected to incident wave pressure amplitudes for planar detonation reflection. Locations and conditions correspond to those used in the experiment described in Fig. 4

x/L	P_2/P_1 (exp)	P_2/P_1 (calc)
0.898	1.30	1.39
0.937	1.59	1.66
0.976	1.96	2.00
1.000	2.65	2.50

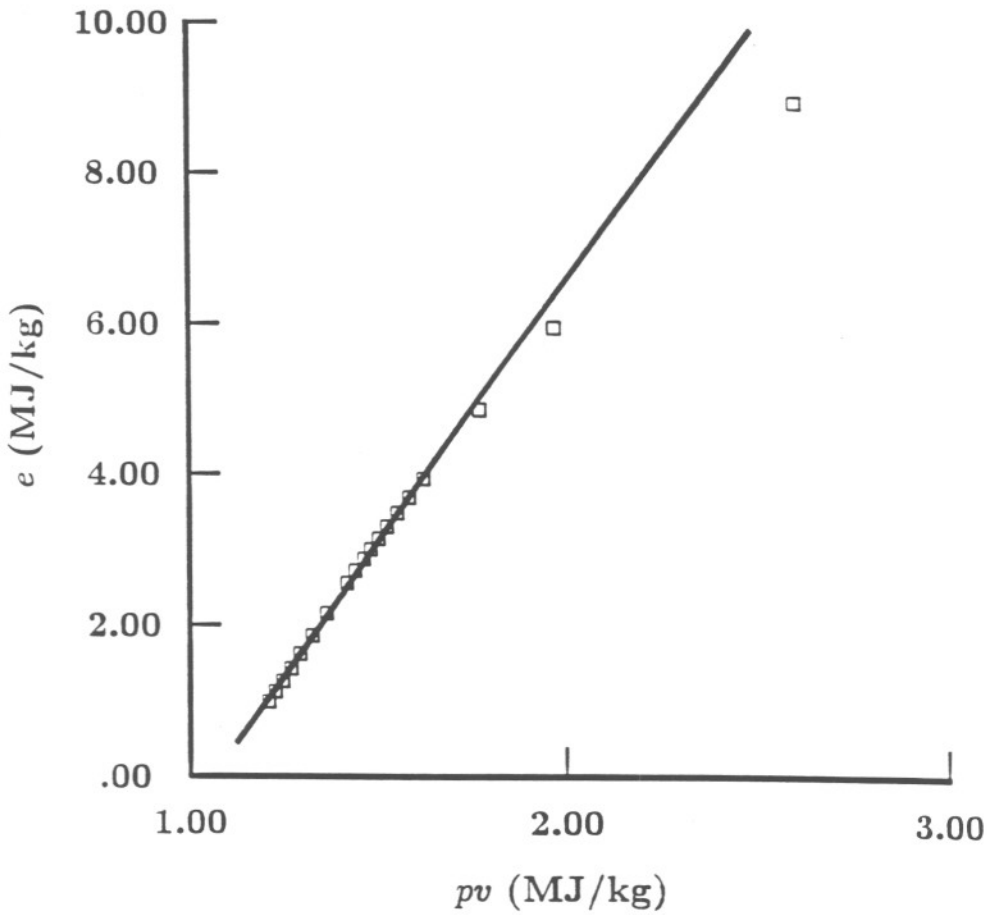

Figure 2. Internal energy e vs. the pressure-volume product pv on the product isentrope passing through the CJ detonation point for a stoichiometric acetylene-oxygen detonation, initial pressure 250 torr, initial temperature 300 K. Data points are the results of STANJAN computations using realistic product thermochemistry, lowest point is at 2 atm, the highest at 500 atm. Line is the least-squares fit of the ideal gas model with $\gamma = 1.1414$, using only data points corresponding to pressures between 5 and 25 atm, i.e., $1.2 < pv < 1.7$ MJ/kg.

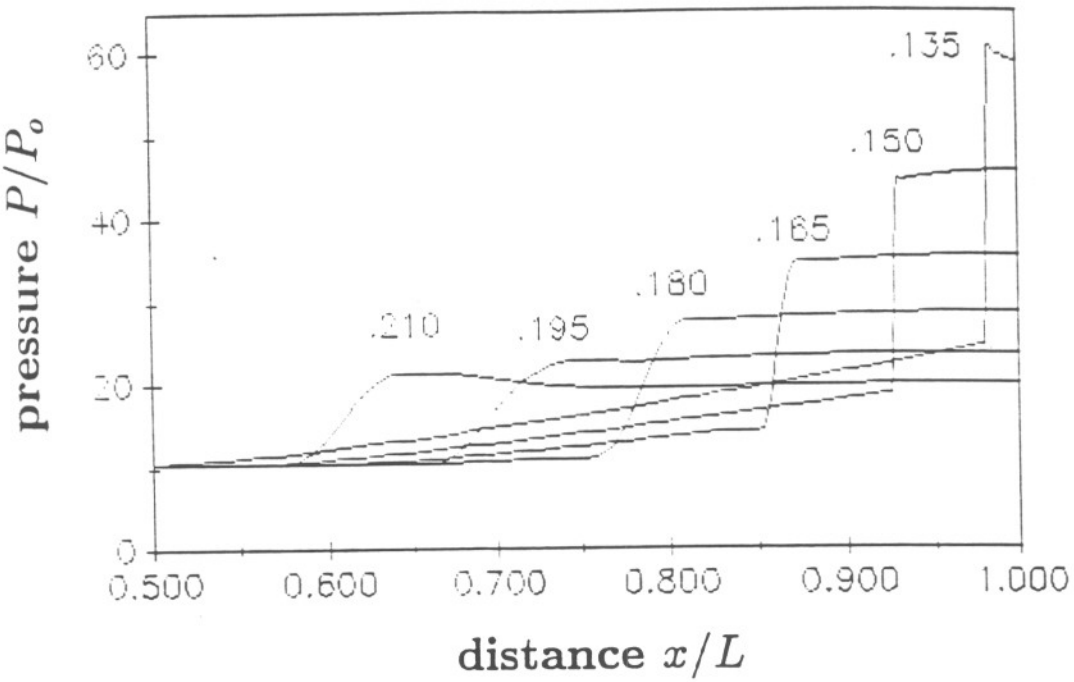

Figure 3. Reflection of a planar detonation from the tube end wall. Pressure P/P_o vs. distance x/L at selected times. Ideal computation (no losses, $C_f = C_h = 0$) using a variable mesh with a total of 250 points. Times are nondimensional $t = c_r\tilde{t}/L$ and relative to the initiation of detonation at the opposite end of the tube ($x = 0$). The reference sound speed is $c_r = \gamma p_o/\rho_o$, where $\gamma = 1.1414$; other parameters are chosen to simulate detonation in stoichiometric acetylene-oxygen at an initial pressure of 250 torr and an initial temperature of 300 K. The shock appears to thicken as it moves away from the wall since the grid is ten times coarser for $x/L < 0.8$ than for $x/L > 0.9$. For $0.8 < x/L < 0.9$, successive grid spacings change as in a geometric progression with a constant ratio.

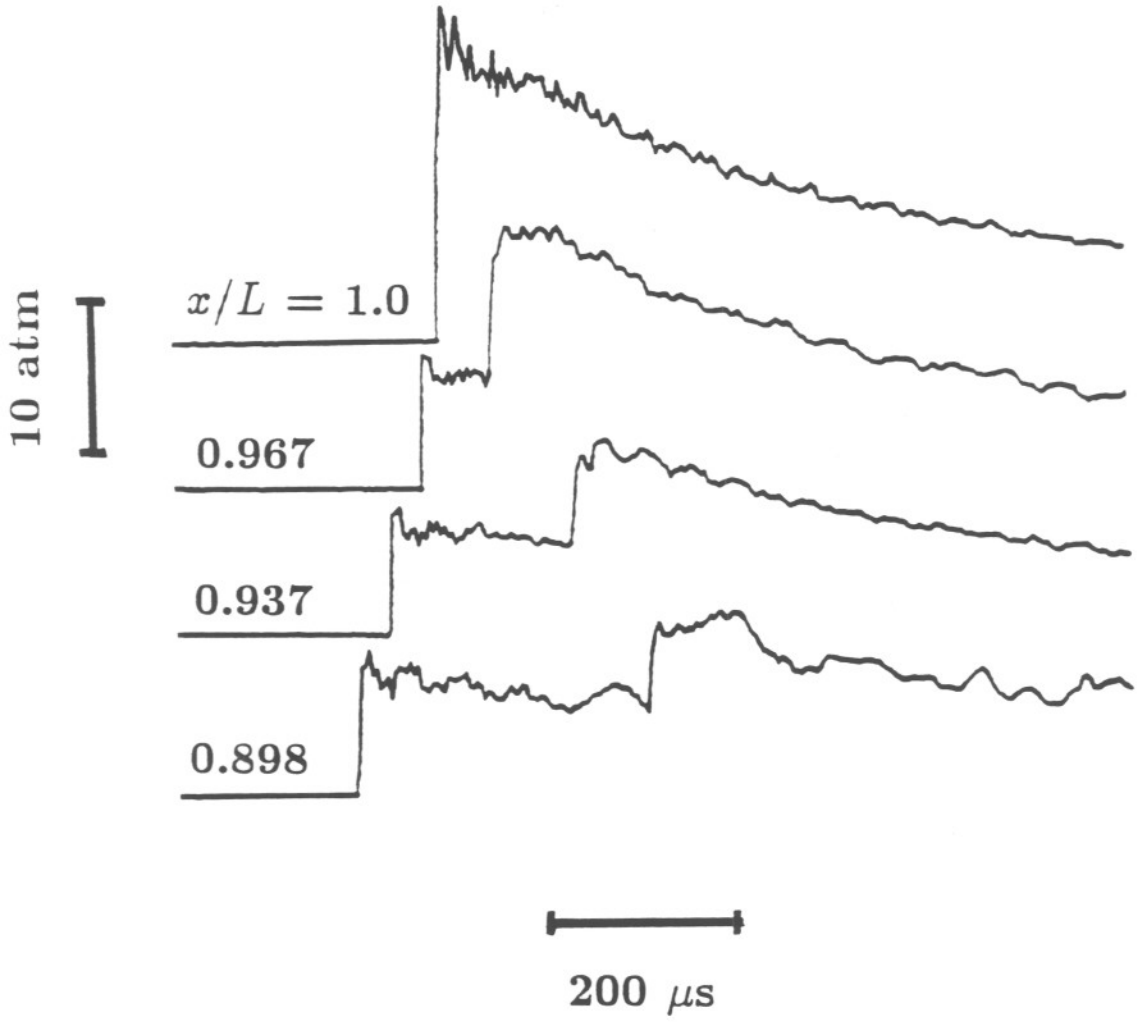

Figure 4. Reflection of a planar detonation from the tube end wall. Experimental results, pressure vs. time at selected locations as shown. Stoichiometric acetylene-oxygen at 200 torr initial pressure, 300 K initial temperature. The vessel was a straight tube 50 mm in diameter and 2.28 m long.

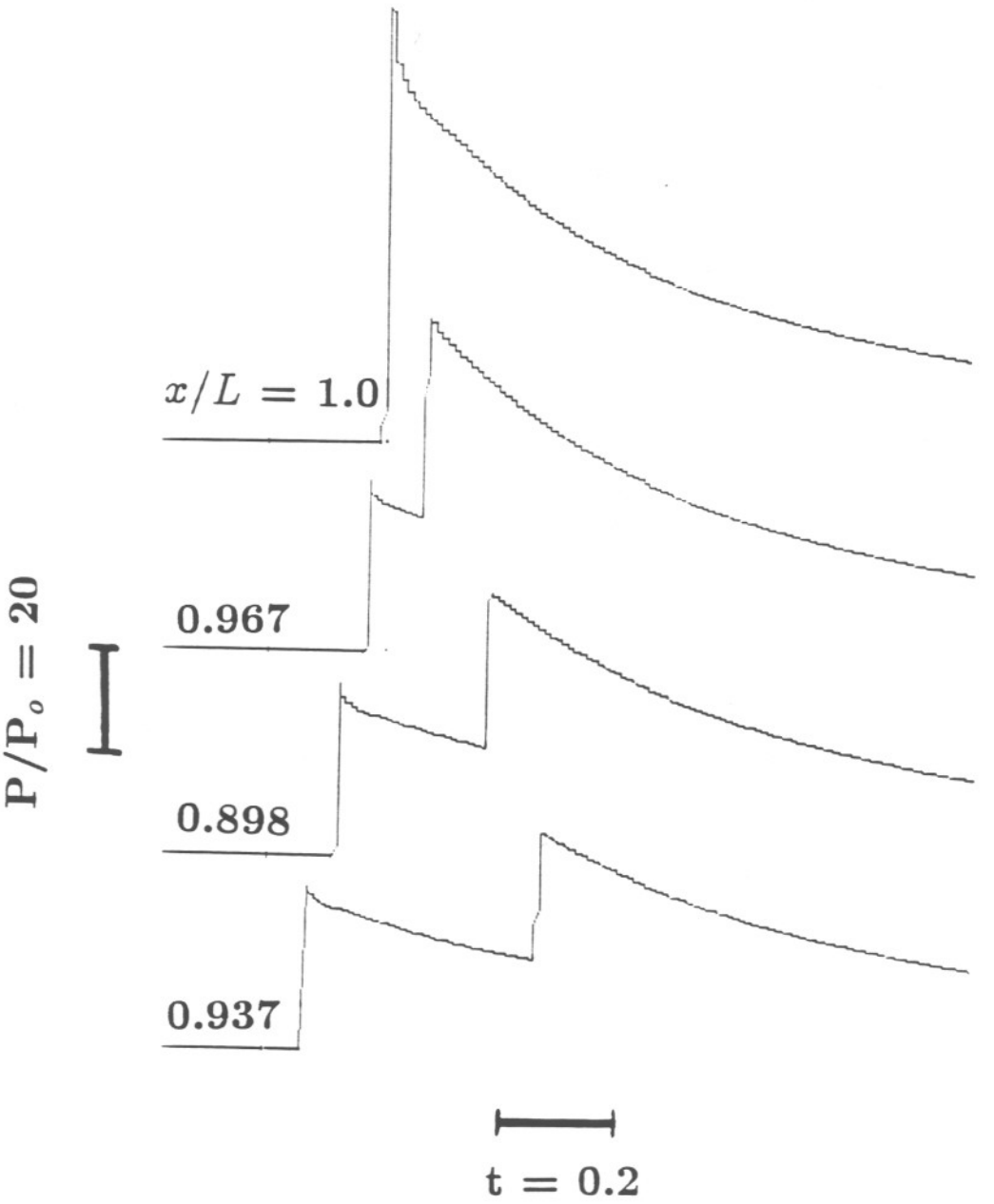

Figure 5. Reflection of a planar detonation from the tube end wall. Numerical simulation (no losses), pressure vs. time at selected locations as shown. Parameters chosen to simulate the conditions for the experimental results shown in Fig. 4. Nondimensional time is $t = c_r\tilde{t}/L$, where c_r = 306.4 m/s and L = 2.28 m.

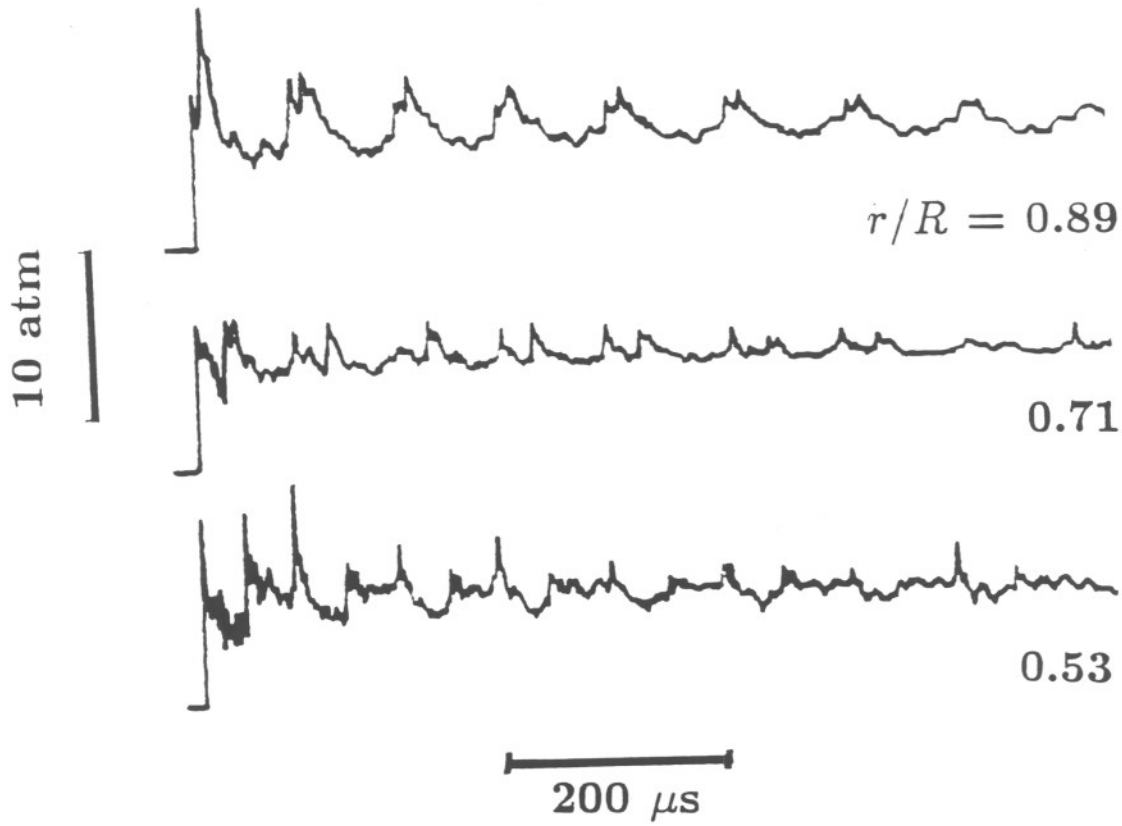

Figure 6. Experimental results in the cylindrical vessel. Pressure vs. time at selected locations as shown. Stoichiometric acetylene-oxygen, initial pressure of 250 torr, initial temperature of 300 K. Vessel radius of 143 mm, thickness of 30.7 mm.

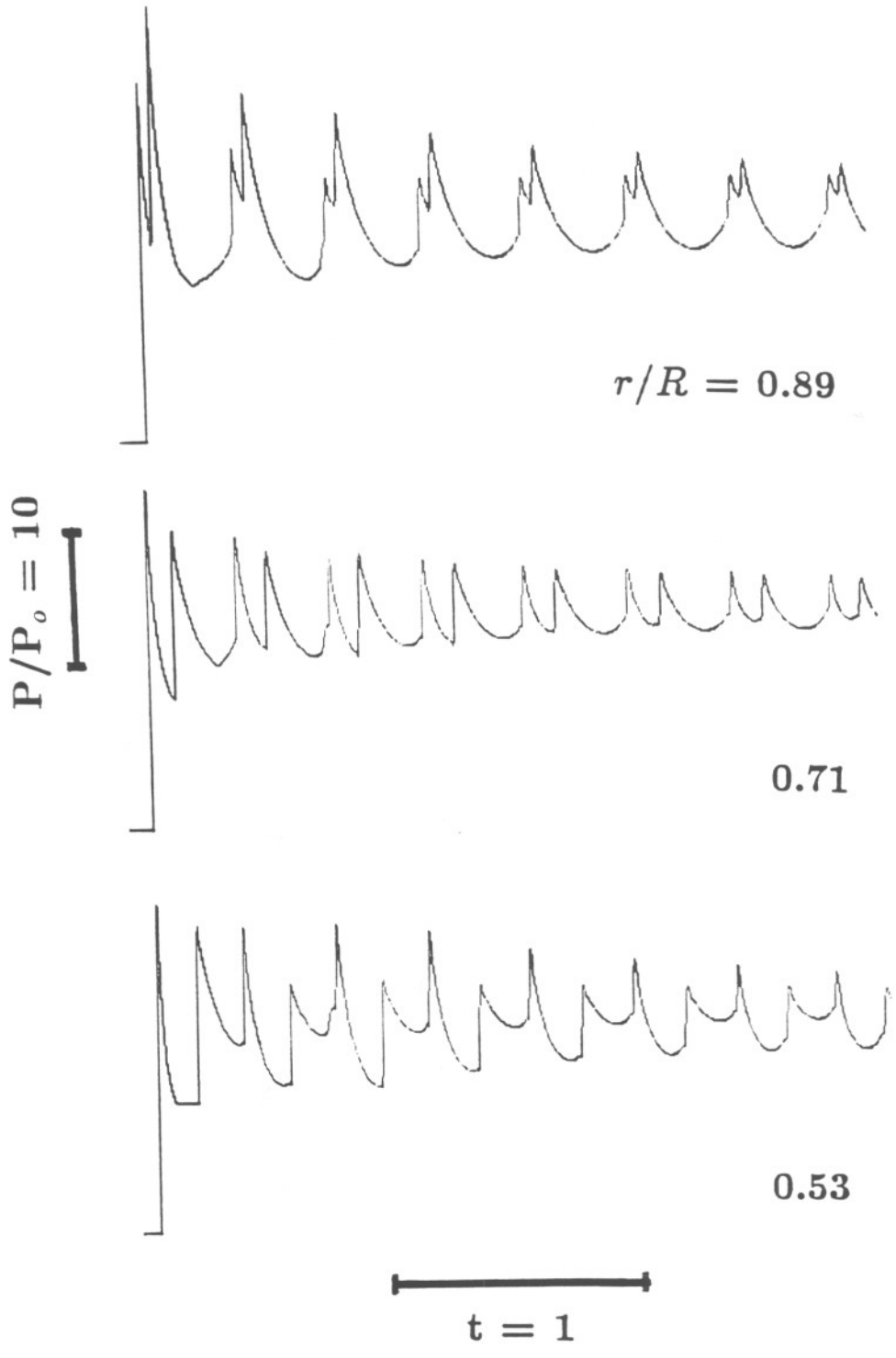

Figure 7. Reflection of a detonation within a cylindrical vessel. Pressure vs. time at selected locations as shown. Numerical results, ideal model (no losses), parameters chosen to simulate the conditions for the experimental results shown in Fig. 6. Nondimensional time is $t = c_r\tilde{t}/R$, where $c_r = 306.4$ m/s and $R = 143$ mm.

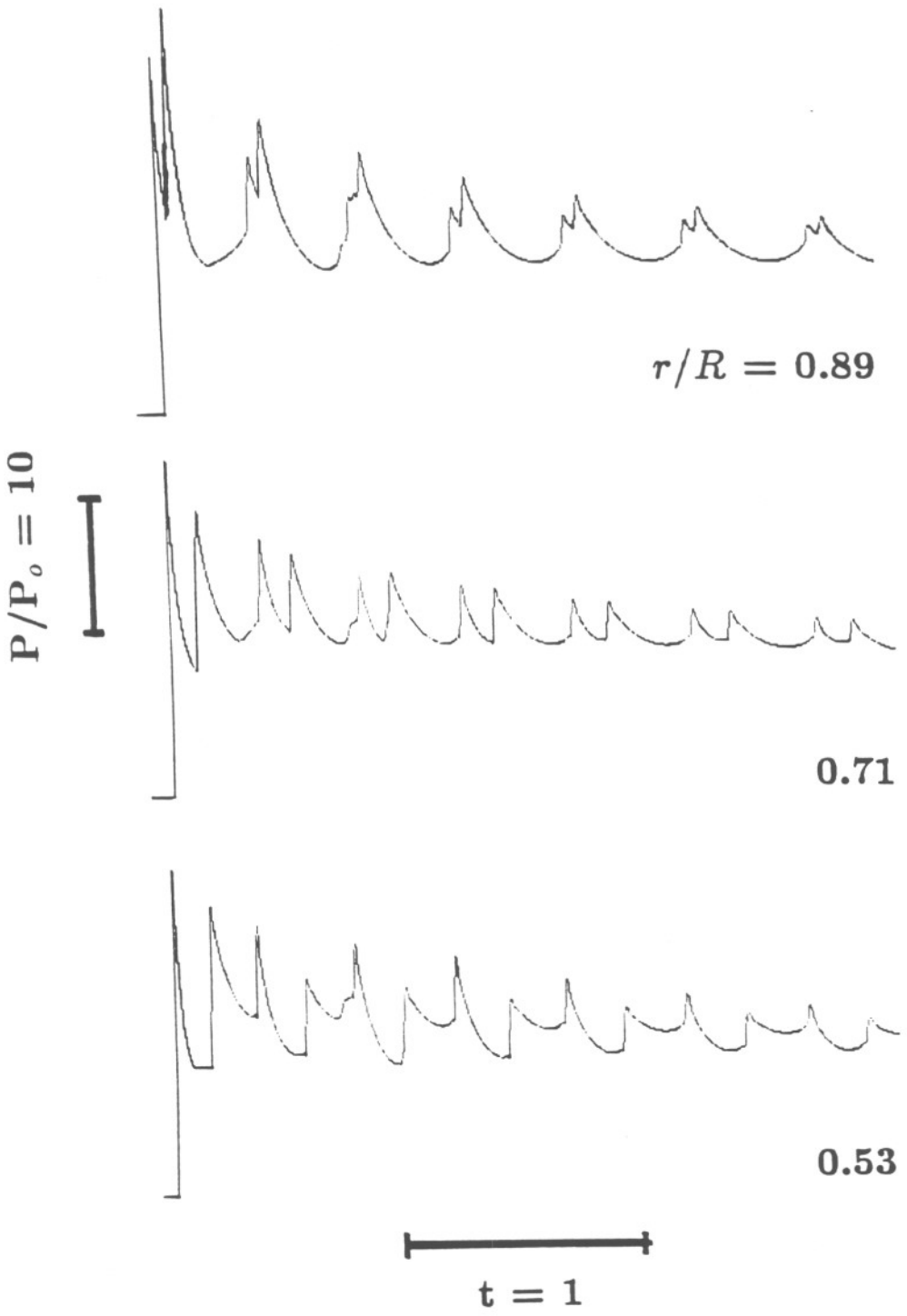

Figure 8. Reflection of a detonation within a cylindrical vessel. Pressure vs. time at selected locations as shown. Numerical results, modeled momentum and energy losses with ad hoc values of transfer coefficients ($C_f = 0.05$, $C_h = 0.025$), other parameters chosen to simulate the conditions for the experimental results shown in Fig. 6. Nondimensional time as defined in Fig. 7.

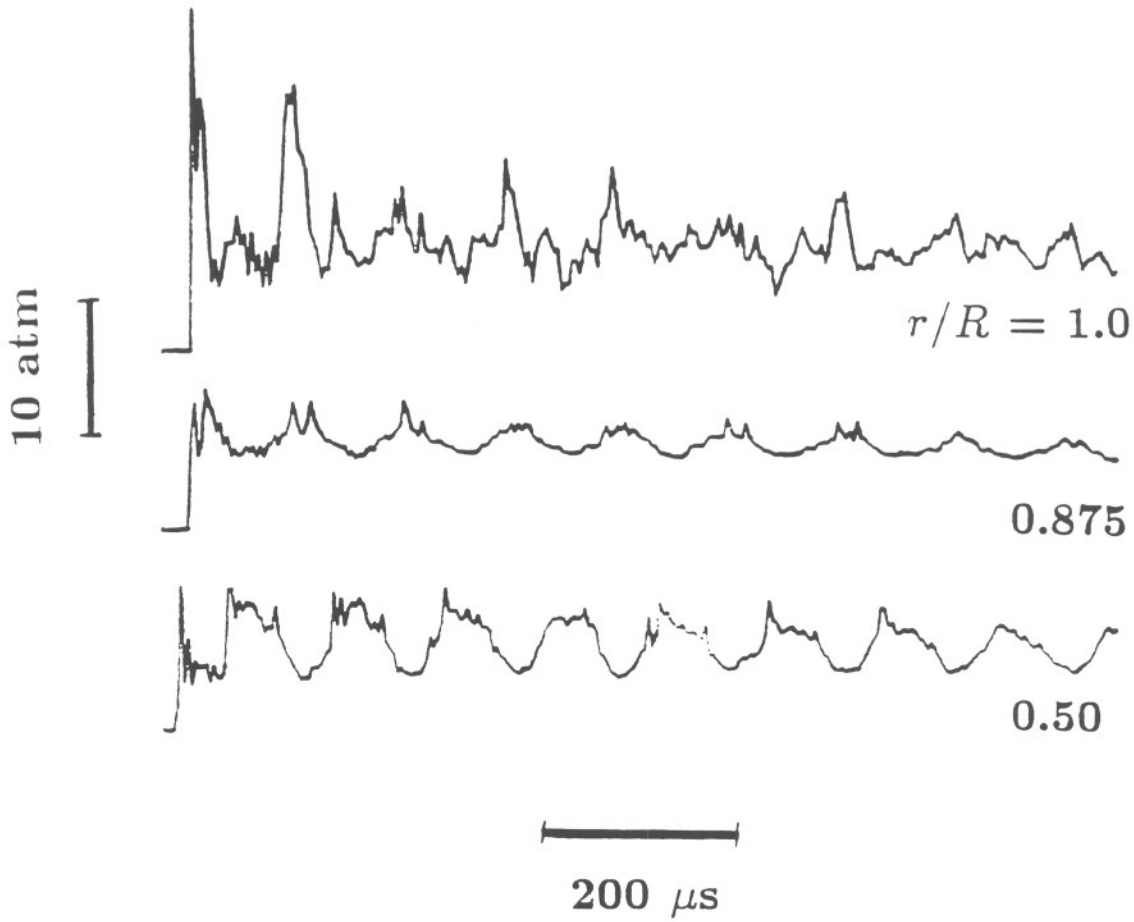

Figure 9. Reflection of a detonation within a hemispherical vessel. Pressure vs. time at selected locations as shown. Experimental results, stoichiometric acetylene-oxygen, initial pressure of 250 torr, initial temperature 300 K. Vessel radius of 102 mm.

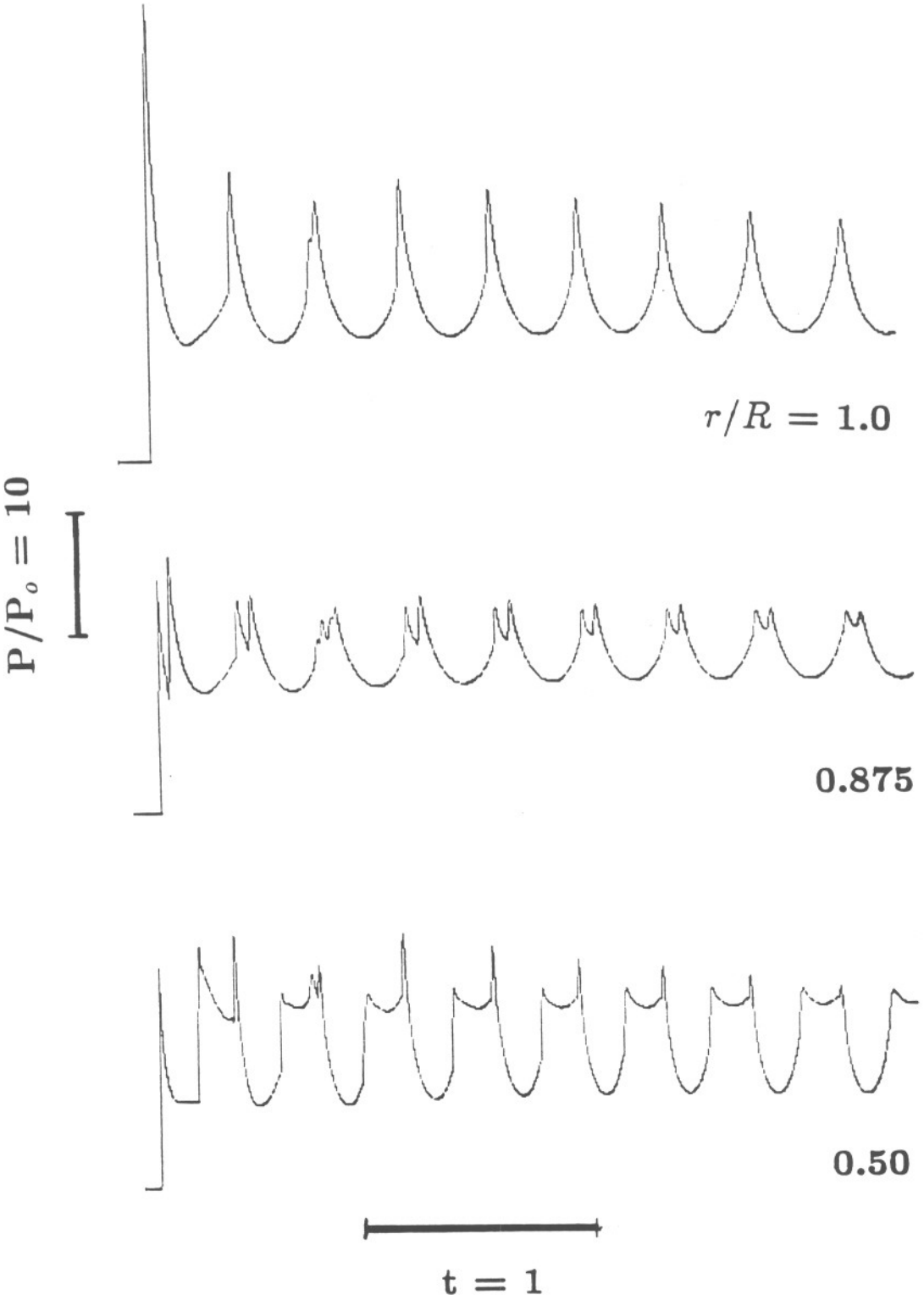

Figure 10. Reflection of a detonation within a hemispherical vessel. Pressure vs. time at selected locations as shown. Numerical results, ideal model (no losses), parameters chosen to simulate the conditions for the experimental results shown in Fig. 9. Nondimensional time is $t = c_r\tilde{t}/R$, where $c_r = 306.4$ m/s and $R = 102$ mm.